Scientific Reports

https://doi.org/10.1038/s41598-026-38233-z

Article in Press

Network and molecular insights into the antidiabetic potential of squalene in alloxan-induced diabetes

Received: 28 September 2025

Accepted: 29 January 2026

Published online: 13 February 2026

Cite this article as: Jaafar F.R., Nassir E.S., Oraibi A.I. *et al.* Network and molecular insights into the antidiabetic potential of squalene in alloxan-induced diabetes. *Sci Rep* (2026). https://doi.org/10.1038/s41598-026-38233-z

Farrah Rasool Jaafar, Eman Sadiq Nassir, Amjad Ibrahim Oraibi, Ali Almukram & Hany Akeel Al-Hussaniy

Network and Molecular Insights into the Antidiabetic Potential of Squalene in Alloxan-Induced Diabetes

Farrah Rasool Jaafar[1], Eman Sadiq Nassir[2], Amjad Ibrahim Oraibi[3*], Ali Almukram[4], Hany Akeel Al-Hussaniy[5]

1- Department of Pharmacology, College of Medicine, AL-Nahrain University, Baghdad City, Iraq 10001
2- Department of clinical laboratory sciences College pf pharmacy / university of baghdad / Baghdad/ Iraq
3- Al-Manara College For Medical Sciences, University of Manara, Maysan, 62001, Iraq
4- University of Maryland, Baltimore, United States of America
5- Department of pharmacy, Al-Nisour University College, Baghdad, Iraq

Corresponding author:

Dr. Amjad Ibrahim Oraibi

Department of Pharmacy, Al-Manara College for Medical Sciences, Maysan, 62001, Iraq

Email id: Amjadibrahim@uomanara.edu.iq

Structured Abstract

Squalene is known for its antioxidant and lipid-lowering effects, and some studies have suggested its antidiabetic potential. This study evaluated the effects of squalene in rats with alloxan-induced type 1 diabetes. Twenty-four rats were divided into four groups: healthy control, alloxan control, and two treatment groups receiving squalene at 100 mg/kg and 200 mg/kg for 30 days. Blood glucose, HbA1c, insulin, lipid profile, kidney function (creatinine), liver glycogen, antioxidant markers (malondialdehyde, superoxide dismutase, glutathione), and pro-inflammatory cytokines (IL-1β, IL-6, TNF-α) were measured. Squalene improved blood glucose control, insulin levels, and lipid profile. It also restored liver glycogen, reduced oxidative stress, and lowered inflammation markers. These effects were more prominent at the higher dose. In addition, network pharmacology and molecular docking analyses identified relevant targets involved in glucose regulation, lipid metabolism, and immune signaling. Squalene showed favorable binding interactions with key proteins such as IL1R1 and

SQLE, supporting its role in modulating both inflammatory and metabolic pathways. Squalene showed beneficial effects in diabetic rats by improving metabolic, antioxidant, and inflammatory parameters. These results suggest that squalene may be a useful compound for supporting diabetes management, and further studies are needed to explore its potential.

Keywords: Squalene, antidiabetic, alloxan-induced diabetes, diabetic model, docking

1. Introduction

Diabetes mellitus is a long-term metabolic disorder that results in elevated blood sugar levels, mainly because the body cannot produce enough insulin or use it effectively. It affects more than 500 million individuals worldwide and continues to rise due to changes in lifestyle, diet, and urbanization[1]. Long-term hyperglycemia in diabetes leads to widespread metabolic derangements and damage to multiple organs, including the eyes, kidneys, liver, and cardiovascular system[2,3]. Among these complications, dyslipidemia, oxidative stress, and chronic inflammation are key contributors to disease progression and comorbidities such as atherosclerosis, retinopathy, nephropathy, and neuropathy[4–6]. The pathophysiology of diabetes involves complex alterations in lipid, carbohydrate, and protein metabolism. One of the critical outcomes of this imbalance is the generation of reactive oxygen species (ROS), which exceed the body's natural antioxidant defense mechanisms. persistent excessive oxidative stress significantly increases the risk of beta cell failure by promoting cell death and reducing insulin production[5–9].The onset and progression of diabetes and its related complications are strongly influenced by oxidative stress and the triggering of inflammatory pathways.

Diabetes is primarily classified into two types: Type 1 diabetes mellitus (T1DM) and Type 2 diabetes mellitus (T2DM). This condition is associated with disruptions in carbohydrate, lipid, and protein metabolism due to insulin deficiency. Insulin deficiency can arise from either impaired insulin production by beta Langerhans cells in the pancreas gland or a lack of

insulin responsiveness in the body cells. T1DM is an autoimmune condition marked by the destruction of insulin-producing pancreatic β-cells, leading to absolute insulin deficiency[10,11]. In contrast, T2DM is typically associated with insulin resistance and relative insulin deficiency, often linked to obesity and metabolic syndrome. While insulin therapy remains the mainstay of treatment for T1DM, it does not fully prevent long-term complications, and alternative or adjunct therapeutic strategies are still under investigation[12–14]. Despite advancements in diabetic management, current pharmacological options are limited by several drawbacks, including adverse side effects, variable patient response, and limited efficacy in preventing disease progression. Moreover, synthetic drugs may contribute to hepatic or renal toxicity when used long-term. As a result, there is growing interest in identifying natural compounds with antidiabetic, antioxidant, and anti-inflammatory properties that may serve as safer alternatives or complements to existing treatments[15,16].

Squalene is a naturally occurring triterpene hydrocarbon that serves as a precursor in the biosynthesis of cholesterol, steroid hormones, and fat-soluble vitamins. Squalene is a natural organic compound obtained for commercial purposes primarily from shark liver oil, although it can also be extracted from botanic sources, including olive oil, palm oil, wheat-germ oil, amaranth oil and rice bran[17,18]. Squalene has been tested widely in pharmacological activity including anticancer, anti-inflammatory, antioxidant, and antidiabetic properties[19]. Several studies have shown that dietary squalene improves lipid profiles by reducing total cholesterol (TC) and triglycerides (TG), and increasing high-density lipoprotein (HDL) levels. These benefits suggest a possible role for squalene in modulating metabolic processes that are disrupted in diabetes[18]. Although some studies have reported the antidiabetic effects of squalene, most of these have used streptozotocin-induced models of diabetes, which primarily mimic Type 2 diabetes or chemically induced β-cell damage[20,21]. The mechanisms through which squalene may exert antidiabetic effects, especially in autoimmune-mediated T1DM models, remain poorly understood. Furthermore, the literature lacks comprehensive evaluations

of squalene in alloxan-induced diabetic models. Alloxan is a toxic glucose analog that selectively destroys pancreatic β-cells by generating ROS, making it a well-established model for simulating Type 1 diabetes in animals. The use of this model allows for the investigation of therapeutic agents that may protect or regenerate β-cell function, regulate glucose metabolism, and modulate inflammatory or oxidative pathways[22–24]. Given this gap in the literature, the present study was designed to evaluate the antidiabetic potential of squalene in an alloxan-induced diabetic rat model. The primary objective was to assess the effects of squalene on blood glucose regulation, insulin secretion, lipid profile, antioxidant enzyme activity, and pro-inflammatory cytokine expression. To complement the in vivo findings, a systems-based computational approach was employed to identify relevant molecular targets and pathways influenced by squalene. Two proteins of particular interest are squalene epoxidase (SQLE) and interleukin-1 receptor type 1 (IL1R1). SQLE is a key enzyme in the cholesterol biosynthesis pathway and a recognized target for lipid-lowering therapy, making it pertinent to metabolic regulation in diabetes[25]. IL1R1, on the other hand, mediates proinflammatory signaling and plays a critical role in autoimmune β-cell destruction in T1DM[26]. Investigating the interaction of squalene with these targets may help elucidate its mechanistic role in modulating metabolic and immune responses. This integrative strategy not only supports the experimental findings but also offers mechanistic insights into squalene's potential therapeutic role in the management of T1DM.

This study is distinct from previous work as it provides the first integrated evaluation of squalene in an alloxan-induced Type 1 diabetes model combined with systems-based network pharmacology and molecular docking analysis. Additionally, multiple interconnected biochemical parameters, glycemic, lipid, antioxidant, renal, pancreatic, and cytokine markers were evaluated simultaneously, offering a broader mechanistic understanding than previously reported investigations.

2. Methods and Materials

2.1. Chemicals and Reagents

Alloxan monohydrates and squalene were purchased from Sigma-Aldrich, USA. Assay kits for creatinine, malonaldehyde (MDA), superoxide dismutase (SOD), glutathione (GSH), and catalase were procured from Iraq Biotech Enzyme-linked immunosorbent assay (ELISA) kits for insulin, IL-1β, IL-6, and TNF-α were obtained from SAMA BAGHDA Scientific company.

2.2. Animals, Housing Conditions, and Ethical Approval

Male Wistar rats (9–10 weeks old, weighing approximately 180 ± 20 g) were obtained. The animals were kept in a controlled environment with a 12-hour light/dark cycle, a temperature of 24 ± 2°C, and relative humidity ranging between 50% and 60%. They had free access to standard pellet food and clean drinking water. Before beginning the experiments, the rats were acclimated to laboratory conditions for one week. All experimental procedures were conducted by trained personnel in accordance with the ARRIVE guidelines and institutional regulations. Ethical approval for the study was granted (Approval No. MUCM/IAEC/2024/03). All methods were carried out in accordance with relevant national and international guidelines and regulations for the care and use of laboratory animals (CPCSEA guidelines).

Induction of Diabetes and Experimental Design

After getting used to the new environment, all rats were kept without food overnight for about eight hours. DM was induced by intraperitoneal injection of alloxan monohydrate (50 mg/kg body weight). Alloxan monohydrate was dissolved in normal saline to achieve a concentration of 5% (W/V) before injection of each rat. To avoid low blood sugar after the injection, each cage had 5% glucose solution for the next 24 hours.[27]. After 72 hours, blood sugar levels were checked using a digital glucometer (ACCU-CHECK, Roche). Rats with blood sugar levels higher than 250 mg/dL were considered diabetic and included in the experiment. A total of 24 rats were randomly divided into four groups, with six rats in

each group. The first group was the health control and did not receive any treatment. The second group included diabetic rats that were not treated and served as disease control. The third and fourth groups were diabetic rats treated with squalene at doses of 100 mg/kg and 200 mg/kg body weight, administered orally once daily for 30 days, and were selected based on previously published pharmacological studies demonstrating safety and therapeutic relevance in metabolic disorders. A preliminary tolerability assessment was conducted before the main study (data not presented here), and no behavioral abnormalities or adverse effects were observed at the selected doses. Body weight and fasting blood glucose levels were measured on Day 0 (before treatment) and again on Days 10, 20, and 30. At the end of the study, blood was collected from the retro-orbital plexus under light isoflurane anesthesia for biochemical testing. The rats were then euthanized humanely by gradual CO_2 inhalation in a controlled euthanasia chamber (Harvard Apparatus, USA) at a flow rate of approximately 20% of the chamber volume per minute, followed by cervical dislocation to confirm death. This method was performed in accordance with the AVMA Guidelines for the Euthanasia of Animals (2020) and the CPCSEA guidelines to ensure minimal pain and distress.

2.3. Biochemical Estimations

Fasting blood glucose levels were measured using a glucometer (ACCU-CHECK, Roche) by collecting blood from the tail vein on Days 0, 10, 20, and 30 of the study periods. For glycated hemoglobin (HbA1c) analysis, blood was drawn from the retro-orbital plexus into tubes containing 0.2% EDTA and mixed with normal saline. Blood samples were processed by centrifugation at 1500 g for 20 minutes at 4°C to separate the serum. HbA1c concentrations were measured using high-performance liquid chromatography (HPLC), following previously established protocols [28]. Serum insulin, amylase, catalase, total cholesterol, triglycerides, and HDL-cholesterol were quantified using a rat-specific ELISA kit, adhering to the supplier's instructions. To determine hepatic glycogen levels, liver tissues were excised, weighed, and homogenized in 5% potassium hydroxide. The

mixture was heated to facilitate glycogen dissolution, followed by ethanol-induced precipitation. The resulting pellet was re-dissolved, and anthrone reagent was added to initiate a colorimetric reaction. Absorbance was recorded at 620 nm, and glycogen content was calculated by referencing a pre-established standard curve [29].

2.4. Renal Function and Antioxidant Enzyme Analysis

Serum creatinine was measured using the modified Jaffe's method, where creatinine reacts with picric acid under alkaline conditions to form a colored complex, detected spectrophotometrically. Liver tissues were rinsed with cold saline, homogenized in 0.1 M Tris-HCl buffer (pH 7.4), and centrifuged to obtain supernatants for antioxidant assays. Superoxide dismutase (SOD) activity was assessed based on the inhibition of NADH-dependent nitro blue tetrazolium reduction, with absorbance recorded at 560 nm[30]. Reduced glutathione (GSH) levels were estimated using Ellman's method, where deproteinized homogenates were treated with Ellman's reagent and disodium hydrogen phosphate, and the resulting yellow complex was measured at 412 nm[31]. Malonaldehyde (MDA), a marker of lipid peroxidation, was quantified using the TBARS assay. The reaction mixture was heated, cooled, extracted with n-butanol and pyridine, and the absorbance of the organic phase was read at 532 nm[32].

2.5. Pro-Inflammatory Cytokine Estimation

To measure the levels of pro-inflammatory cytokines (IL-1β, IL-6, and TNF-α) in serum, ELISA kits designed specifically for rats (Arigo) were used. The assay procedures strictly followed the kit instructions. Each serum sample was tested twice to improve reliability. The intensity of the color reaction was read at the appropriate wavelength using a microplate reader, and cytokine concentrations were calculated using a standard calibration curve provided in the kit[33].

2.6. Statistical Analysis

All data are presented as mean ± standard deviation (SD) for six animals per group. Statistical comparison between disease group and other groups

were made using one-way ANOVA followed by Tukey's post hoc test. A p-value of less than 0.05 was considered statistically significant. GraphPad Prism Software (v5 GraphPad, USA) was used for all statistical analyses

2.7. Systems-Based Clustering and Network Analysis

Target genes for squalene were retrieved from the STITCH database by selecting only experimentally supported and high-confidence interactions[34]. To identify diabetes-relevant overlaps, T1DM-associated genes were compiled from GeneCards (15,162 genes) and OMIM (207 genes)[35,36]. Common genes between squalene targets and T1DM were identified using a Venn diagram analysis. Protein–protein interaction (PPI) data for the common genes were analyzed using the STRING database (v12), with a minimum required interaction score of 0.4[37]. The resulting network was subjected to k-means clustering (k=3) using STRING's internal clustering module. Each cluster was functionally annotated based on GO terms and pathway descriptions automatically provided by STRING. To further characterize biological relevance, functional enrichment was performed using Metascape[38], focusing on GO Biological Processes, Reactome, KEGG[39,40], WikiPathways, and InterPro Domains. Graph-based visualizations were generated from Metascape outputs to represent each enrichment category with similarity grouping.

2.8. Molecular Docking

Molecular docking was performed to study how squalene binds to two target proteins: interleukin-1 receptor type 1 (IL1R1, PDB ID: 1ITB)[41] and squalene epoxidase (SQLE, PDB ID: 6C6N)[42]. The 3D structures of both proteins were downloaded from the Protein Data Bank. All water molecules and existing ligands were removed, and hydrogen atoms were added. Energy minimization was done using Swiss-PdbViewer to clean and optimize the protein structures. The structure of squalene (PubChem CID: 638072) was downloaded and converted into PDBQT format using Open Babel. The molecule was energy-minimized and prepared in AutoDock Tools, where torsions were set and charges were added[43].

Docking was carried out using AutoDock Vina. A grid box was set to cover the active site of each protein based on known binding regions. Binding interactions were visualized using PyMOL to identify key residues involved. These interactions were compared with those reported in the literature to confirm binding at relevant sites.

3. Results

3.1. Effect of Squalene on Body Weight

Weight measurements were taken at the beginning and end of the study (Day 0 and Day 30) and were used to assess the weigh difference in the experimental groups. Rats administered with alloxan showed a significant decrease in body weight by Day 30 ($p < 0.001$), which aligns with the known pattern of weight loss commonly associated with diabetic conditions (**Figure 1**). However, treatment with squalene at both 100 and 200 mg/kg effectively mitigated this effect, as no significant reduction was observed in body weight at the end of the treatment period compared to baseline. This suggests that squalene administration may help preserve body weight in diabetic conditions.

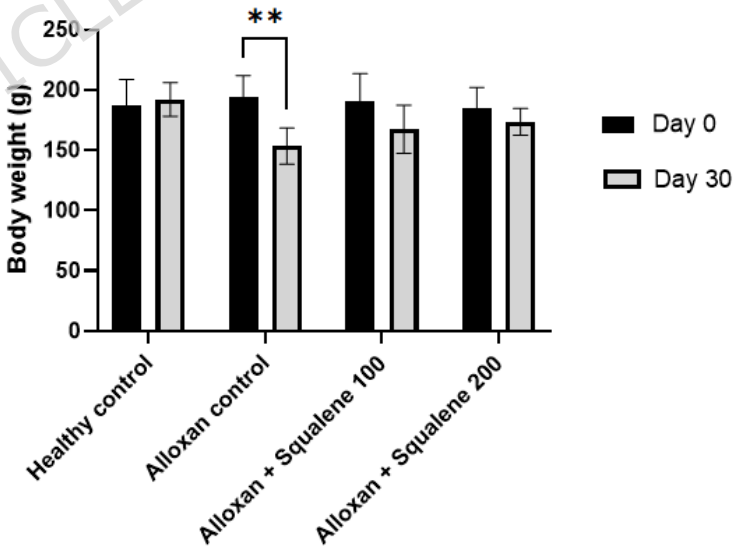

Figure 1. Effect of squalene treatment on body weight changes observed on Day 0 and Day 30. $p < 0.001$.

3.2. Effect of Squalene on HbA1c and Fasting Blood Glucose Levels

Hemoglobin A1c is a critical indicator of long-term glycemic control. In this study, alloxan-induced diabetic rats exhibited a marked increase in HbA1c levels compared to the healthy control group ($p < 0.0001$), confirming persistent hyperglycemia. Treatment with squalene produced a dose-dependent improvement. Squalene at 100 mg/kg led to a significant reduction in HbA1c ($p < 0.05$), while the 200 mg/kg dose resulted in a more substantial decrease ($p < 0.0001$). Notably, HbA1c levels in the 200 mg/kg group approached those of the healthy control, indicating effective long-term glucose regulation. In parallel, fasting blood glucose was assessed on Days 0, 10, 20, and 30. Alloxan treatment caused a sustained and significant elevation in glucose levels at all time points when compared to healthy controls ($p < 0.0001$). Squalene administration led to a progressive, dose-dependent decrease in fasting glucose. By Day 10, the 200 mg/kg dose significantly lowered glucose levels ($p < 0.05$), with further reductions noted on Day 20 for both 100 mg/kg ($p < 0.05$) and 200 mg/kg ($p < 0.001$). At Day 30, both doses resulted in substantial improvement, with 100 mg/kg ($p < 0.001$) and 200 mg/kg ($p < 0.0001$) groups demonstrating significantly lower glucose compared to the diabetic control (**Figure 2**). These findings suggest that squalene contributes to both short-term and sustained glycemic control.

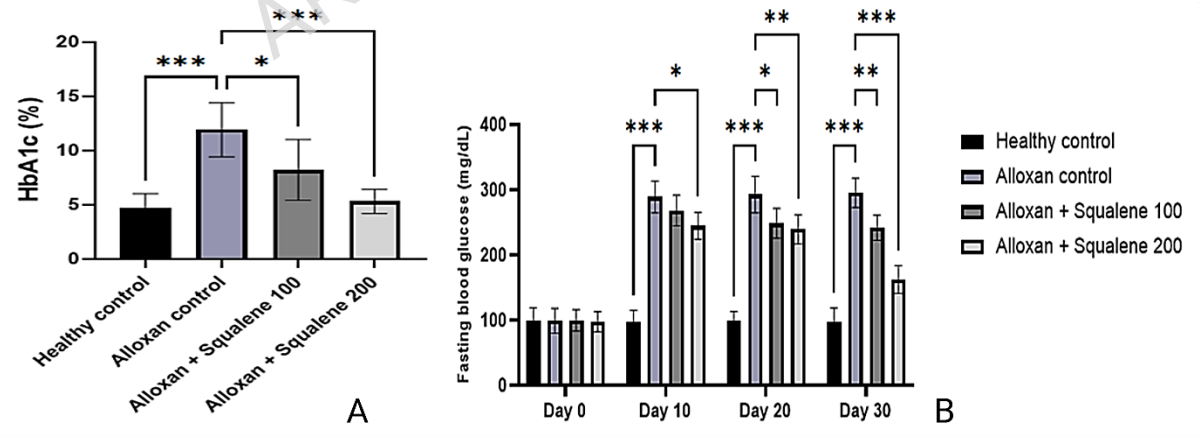

Figure 2: Effect of squalene on (A) HbA1c levels and (B) fasting blood glucose in alloxan-induced diabetic rats. Values are presented as mean ± SD (n = 6). *p < 0.05, **p < 0.001, ***p < 0.0001.

3.3. Effect of Squalene on Serum Insulin and Amylase Levels

Alloxan administration led to a significant reduction in serum insulin levels ($p < 0.0001$), reflecting β-cell damage and impaired insulin secretion (**Figure 3**). Treatment with squalene markedly reversed this effect. At both 100 mg/kg and 200 mg/kg doses, insulin levels were significantly elevated compared to the diabetic control group ($p < 0.05$ and $p < 0.0001$, respectively). Notably, the higher dose of squalene restored insulin levels closer to those observed in healthy controls, indicating a potential protective effect on pancreatic β-cells and enhancement of insulin secretion. In contrast, serum amylase levels were significantly elevated in the alloxan-induced diabetic rats ($p < 0.0001$), suggesting pancreatic dysfunction and hyperenzymemia (**Figure 3**). Squalene treatment at 100 mg/kg significantly reduced amylase levels ($p < 0.05$), and the 200 mg/kg dose produced a more pronounced decrease ($p < 0.001$), bringing the levels closer to normal. This dose-dependent reduction implies that squalene may help restore pancreatic enzymatic balance by alleviating oxidative stress and preserving pancreatic tissue integrity.

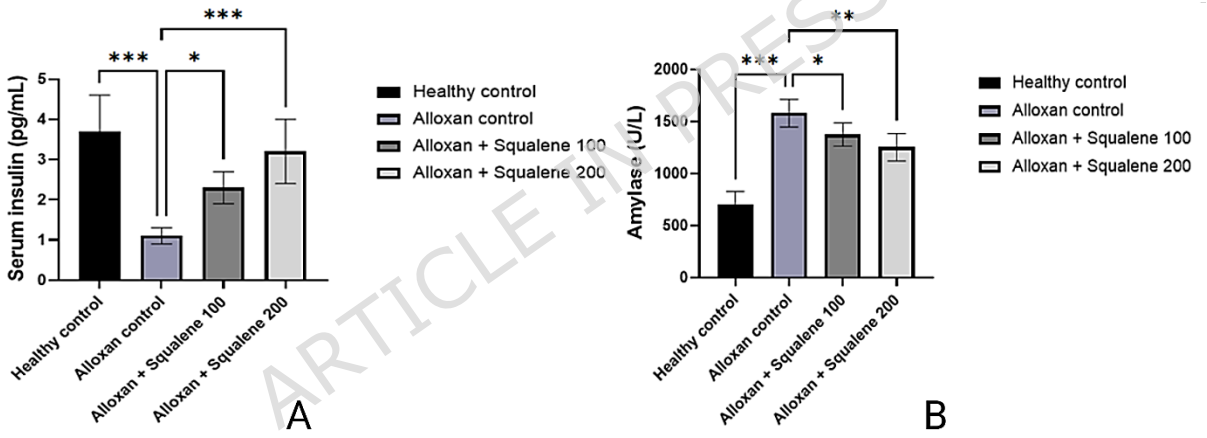

Figure 3: Impact of squalene on (A) serum insulin levels and (B) amylase activity in alloxan-induced diabetic rats. Values are presented as mean ± SD (n = 6). *p < 0.05, **p < 0.001, ***p < 0.0001.

3.4. Effect of Squalene on Lipid Profile and Glycogen Content

Alloxan-induced diabetic rats showed a marked dysregulation of lipid metabolism, characterized by significantly elevated total cholesterol (TC) and triglyceride (TG) levels ($p < 0.0001$), along with a reduction in high-density lipoprotein (HDL) levels ($p < 0.001$), as shown in **Figure 4.** This profile reflects the typical dyslipidemia state associated with diabetes. Treatment with squalene at both 100 mg/kg and 200 mg/kg significantly

lowered TC and TG levels. At 100 mg/kg, reductions in TC and TG were observed ($p < 0.05$), while the 200 mg/kg dose resulted in a more pronounced decrease ($p < 0.001$ for both parameters). HDL levels were also significantly elevated following administration of the higher dose ($p < 0.05$), suggesting a protective effect on lipid metabolism. In parallel, glycogen content in the liver was notably diminished in the diabetic group ($p < 0.001$), indicating disrupted carbohydrate metabolism (**Figure 4**). Squalene supplementation reversed this effect in a dose-dependent manner. The 100 mg/kg dose partially improved glycogen storage ($p < 0.05$), while the 200 mg/kg dose significantly elevated glycogen levels ($p < 0.001$), restoring them close to normal physiological levels. Together, these outcomes highlight the broader metabolic regulatory role of squalene beyond glucose control.

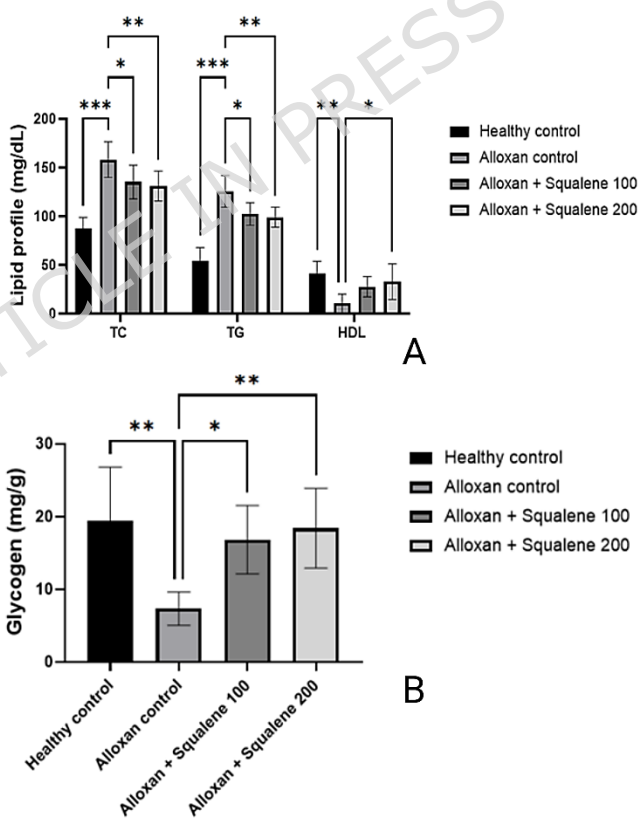

Figure 4. Effect of squalene on (A) lipid profile and (B) liver glycogen content in alloxan-induced diabetic rats. Data are shown as mean ± SD (n = 6). *p < 0.05, **p < 0.001, ***p < 0.0001.

3.5. Effect of Squalene on Serum Creatinine Levels

Alloxan-induced diabetic rats showed a significant elevation in serum creatinine levels compared to the healthy control group ($p < 0.0001$), indicating renal dysfunction associated with hyperglycemia and oxidative damage (**Figure 5**). Squalene treatment at both 100 mg/kg and 200 mg/kg body weight significantly reduced serum creatinine concentrations. The lower dose produced a moderate decrease ($p < 0.001$), while the higher dose showed a more substantial reduction ($p < 0.0001$). This pattern suggests that squalene exerts a protective effect on renal function, likely through its antioxidant and anti-inflammatory mechanisms.

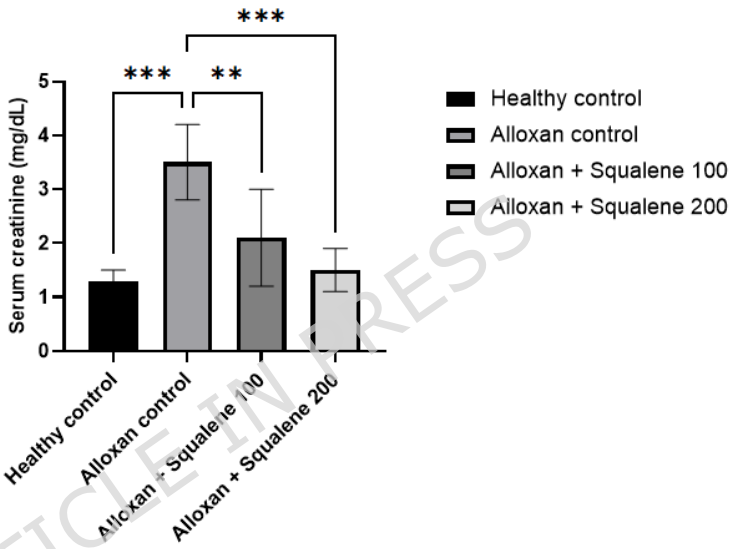

Figure 5: Effect of squalene treatment on serum creatinine levels in alloxan-induced diabetic rats. Data are expressed as mean ± SD (n = 6). **p < 0.001, ***p < 0.0001.

3.6. Effect of Squalene on MDA, SOD and GSH

The antioxidant status was evaluated by measuring levels of malonaldehyde (MDA), superoxide dismutase (SOD), glutathione (GSH), and catalase in liver tissues (**Figure 6A-D**). In alloxan-induced diabetic rats, a significant increase in MDA levels ($p < 0.0001$) indicated enhanced lipid peroxidation, while levels of SOD, GSH, and catalase were markedly reduced ($p < 0.0001$), reflecting compromised antioxidant defenses. Squalene treatment led to a dose-dependent improvement in antioxidant enzyme activity. At 100 mg/kg, MDA levels were significantly reduced

($p < 0.05$), and further suppressed at 200 mg/kg ($p < 0.0001$). SOD activity improved significantly with both doses, with the higher dose restoring levels close to the healthy group ($p < 0.0001$). Similarly, GSH and catalase levels were significantly elevated in squalene-treated groups, with the 200 mg/kg dose showing greater efficacy ($p < 0.001$ for both), suggesting effective mitigation of oxidative stress by squalene in diabetic conditions.

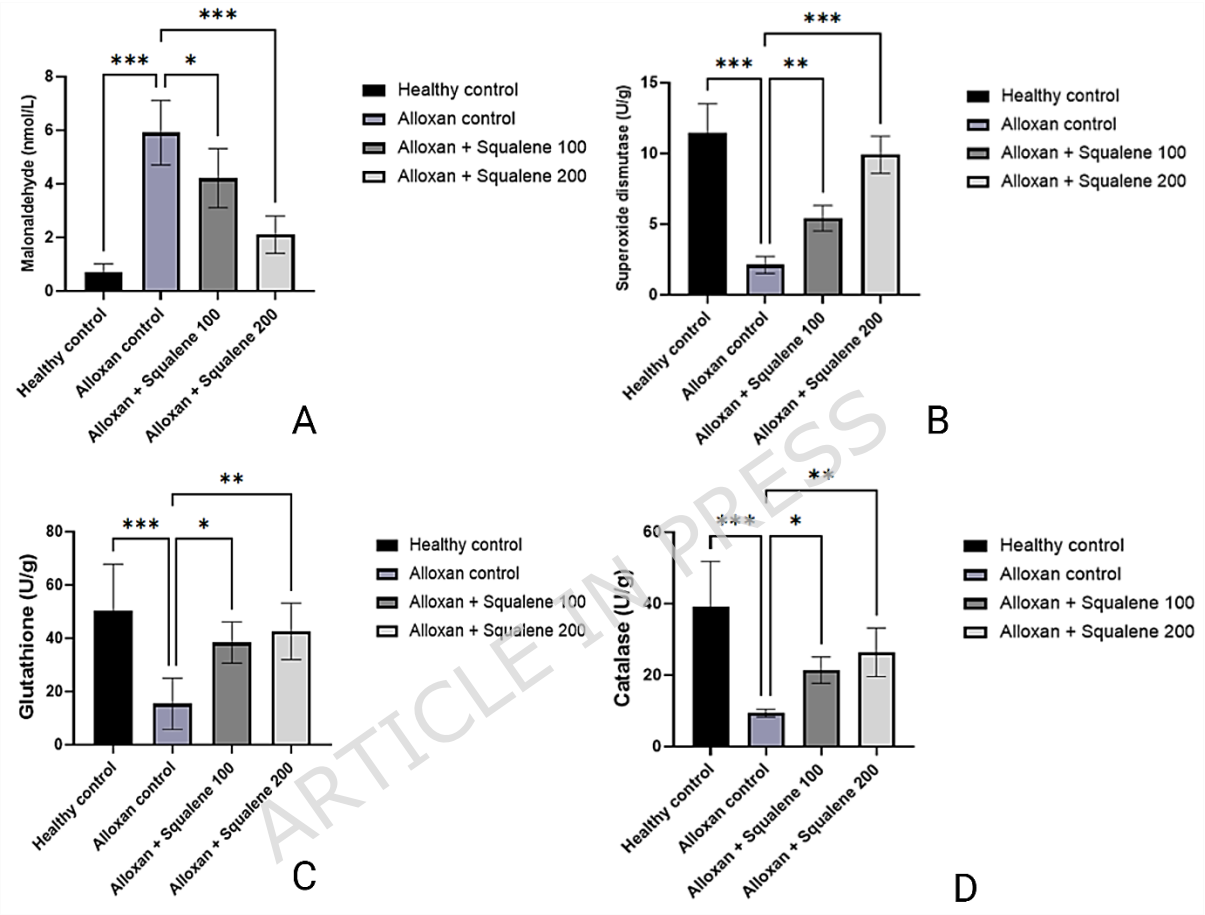

Figure 6: Effect of squalene administration on antioxidant defence markers in diabetic rats: (A) Malondialdehyde (MDA), (B) Superoxide dismutase (SOD), (C) Glutathione (GSH), and (D) Catalase (CAT). Values are shown as mean ± SD (n = 6). *$p < 0.05$, **$p < 0.001$, ***$p < 0.0001$.

3.7. Effect of Squalene on Pro-Inflammatory Cytokines

Serum concentrations of pro-inflammatory cytokines IL-1β, IL-6, and TNF-α were evaluated to determine the extent of the inflammatory response (**Figure 7A-C**). Diabetic rats induced with alloxan showed markedly elevated levels of these cytokines when compared to healthy controls ($p < 0.0001$), confirming the presence of diabetes-related inflammation. Treatment with squalene led to a noticeable decline in cytokine expression,

suggesting its potential to reduce inflammation under diabetic conditions. At 100 mg/kg, IL-1β, IL-6, and TNF-α were all significantly reduced ($p < 0.001$), and further reductions were observed with the 200 mg/kg dose ($p < 0.0001$ for all three cytokines). The higher dose brought cytokine levels closer to the baseline of healthy rats, indicating a substantial anti-inflammatory effect. These results suggest that squalene modulates inflammatory signaling in diabetic pathology by downregulating key cytokines involved in immune-mediated tissue damage.

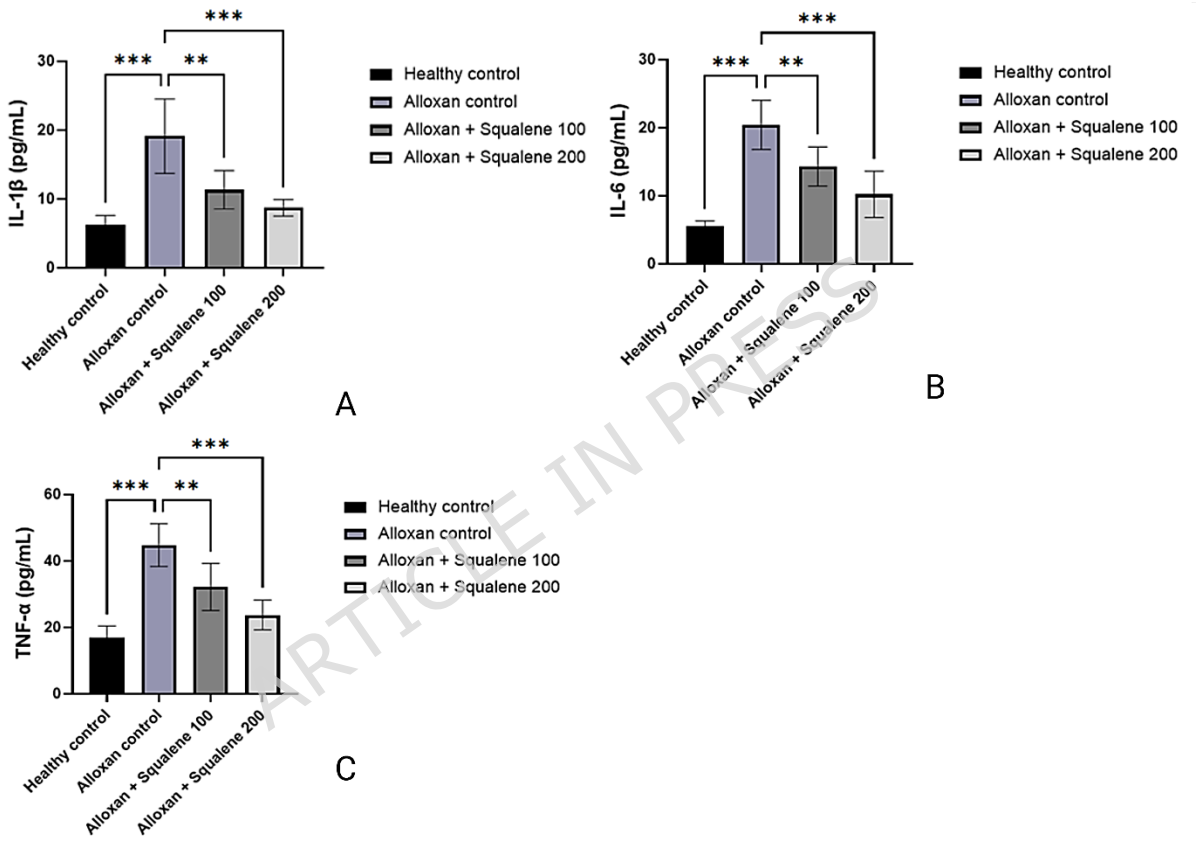

Figure 7: Evaluation of squalene's effect on inflammatory cytokines: (a) IL-1β, (b) IL-6, and (c) TNF-α. Cytokine levels are reported as mean ± SD (n = 6). **p < 0.001, ***p < 0.0001.

3.8. Systems-Based Analysis of Squalene's Mechanism in Type 1 Diabetes

This study employed systems-level computational analysis to explore the potential mechanisms through which squalene may exert therapeutic effects in Type 1 Diabetes Mellitus (T1DM). Using STITCH, nine human

proteins were predicted to interact with squalene. These included chemokines and cytokine regulators (IL1RN, CCL2, CCL3, CCL4, CCL5) and cholesterol biosynthesis enzymes (FDFT1, SQLE, DHCR24, LSS). These targets were compared with genes associated with T1DM obtained from GeneCards (20,087 entries) and OMIM (207 genes) (**Table S1**). All nine squalene targets overlapped with known diabetes-associated genes, suggesting their involvement in the disease's molecular landscape. Gene Ontology (GO) enrichment analysis showed that these targets were strongly associated with biological processes such as immune cell chemotaxis and inflammatory signaling. Among the most significantly enriched processes were the regulation of natural killer (NK) cell, monocyte, neutrophil, and macrophage chemotaxis (**Figure 8)**. These mechanisms play a central role in recruiting immune cells to the pancreatic islets, which is a hallmark of autoimmune β-cell destruction in T1DM. The involvement of CCL2, CCL3, CCL4, and CCL5, along with IL1RN, points to a coordinated immunomodulatory role. Additional enriched terms, including chemokine-mediated signaling, cellular response to interleukin-1, and regulation of cytokine production, further indicate squalene’s potential to influence broader innate immune processes.

On the metabolic side, significant enrichment was found in sterol biosynthetic and cholesterol-related processes. The targets SQLE, DHCR24, FDFT1, and LSS are all part of the SREBP-regulated transcriptional system and play vital roles in maintaining lipid homeostasis. Dysregulation of these pathways has been linked to lipotoxicity and β-cell dysfunction in diabetes. Thus, restoration of these metabolic routes may improve pancreatic health and systemic glucose regulation. Molecular function analysis revealed strong associations with chemokine receptor binding, cytokine activity, and cytokine receptor interactions functional domains known to amplify autoimmune signaling in T1DM (**Figure 8**). For instance, CCL2 and CCL5 interact with CCR2 and CCR5 receptors, respectively, promoting T-cell and macrophage infiltration into pancreatic tissue. These interactions suggest a mechanism

by which squalene could dampen inflammatory cascades by modulating chemokine-receptor binding. Pathway enrichment analysis using Reactome further highlighted the involvement of interleukin-10 signaling, cholesterol biosynthesis, and SREBP-mediated gene activation. IL-10 is an anti-inflammatory cytokine known to promote immune tolerance and limit β-cell destruction (**Figure 8)**. The predicted engagement of squalene with this pathway suggests a capacity to shift the immune response toward a more regulated state. Meanwhile, the enrichment of cholesterol biosynthesis and SREBP activation pathways supports squalene's potential to normalize lipid profiles and mitigate metabolic disturbances. These findings reflect a dual action of squalene on immune and metabolic components of T1DM, consistent with observations from the in vivo portion of the study. All the supporting data are given in Supplementary **Tables S2-S8.**

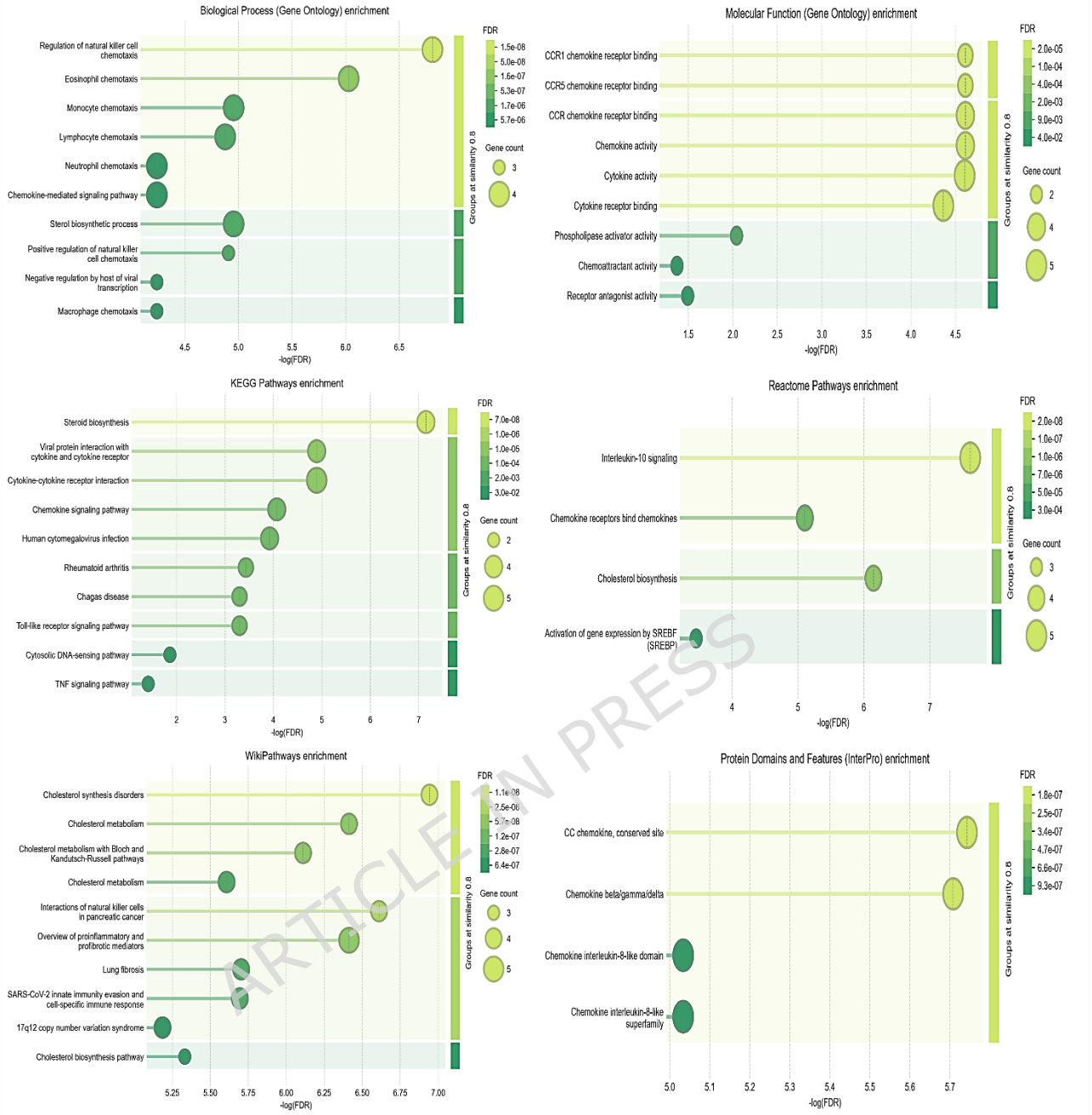

Figure 8: Gene Ontology (GO) annotation analysis highlighting the biological pathways associated with the identified gene set.

3.9. Network Clustering and Functional Module Analysis

Further analysis of the predicted squalene targets using STRING-based network modeling revealed two highly interconnected modules (**Table S9**). The first cluster, composed of IL1RN and the four chemokines CCL2, CCL3, CCL4, and CCL5, showed tight co-expression and was enriched for chemokine signaling functions. The second cluster consisted of metabolic

enzymes SQLE, DHCR24, FDFT1, and LSS, which are responsible for successive steps in sterol and cholesterol biosynthesis (**Figure 9**). These distinct but connected modules illustrate squalene's dual mechanism of action, modulating both immune responses and metabolic pathways relevant to T1DM. KEGG enrichment analysis reinforced these findings, identifying steroid biosynthesis, cytokine–cytokine receptor interaction, and chemokine signaling as key pathways. These processes are central to the development of autoimmune inflammation and the metabolic dysfunction seen in diabetic pathology. Additional support came from WikiPathways, which indicated strong involvement of cholesterol biosynthesis, SREBP signaling, and pathways associated with proinflammatory mediator regulation. Immune-related pathways such as IL-18 and Toll-like receptor signaling were also enriched. Moreover, tissue-specific expression analysis highlighted NK cell-associated mechanisms, aligning with the GO terms and further implicating squalene in modulating immune cell recruitment.

Domain annotation using InterPro and SMART identified conserved structural motifs across squalene targets, including CC chemokine conserved sites and IL-8-like domains, which are typical of immune signaling proteins. UniProt keyword analysis revealed further enrichment in terms related to chemotaxis, cytokine activity, steroid biosynthesis, and inflammatory responses, supporting the observed immune-metabolic connectivity. To dissect these interactions further, k-means clustering was applied to the protein–protein interaction network, revealing three distinct modules. The first included CCL2 through CCL5 and was annotated with regulation of NK cell chemotaxis. These chemokines are known to attract cytotoxic immune cells to pancreatic islets, contributing to β-cell destruction[44]. The second module grouped the metabolic enzymes involved in cholesterol biosynthesis, reflecting squalene's integration into lipid metabolic regulation. This association supports the hypothesis that squalene not only acts as a structural precursor but may also stabilize membrane lipid composition and mitigate β-cell lipotoxicity[45]. The third cluster included IL1RN alone, suggesting a unique and independent role

in dampening interleukin-1–driven cytokine cascades. IL1RN is a natural antagonist of the IL-1 receptor and plays a protective role in autoimmune diabetes models (**Figure 9)**. Thus, these findings provide a systems-level understanding of how squalene may exert protective effects in T1DM by simultaneously modulating immune responses and lipid metabolism. The convergence of chemokine signaling, cytokine regulation, and cholesterol biosynthesis within a unified interaction network underscores squalene's potential to restore balance in both immune and metabolic pathways disrupted during the progression of autoimmune diabetes.

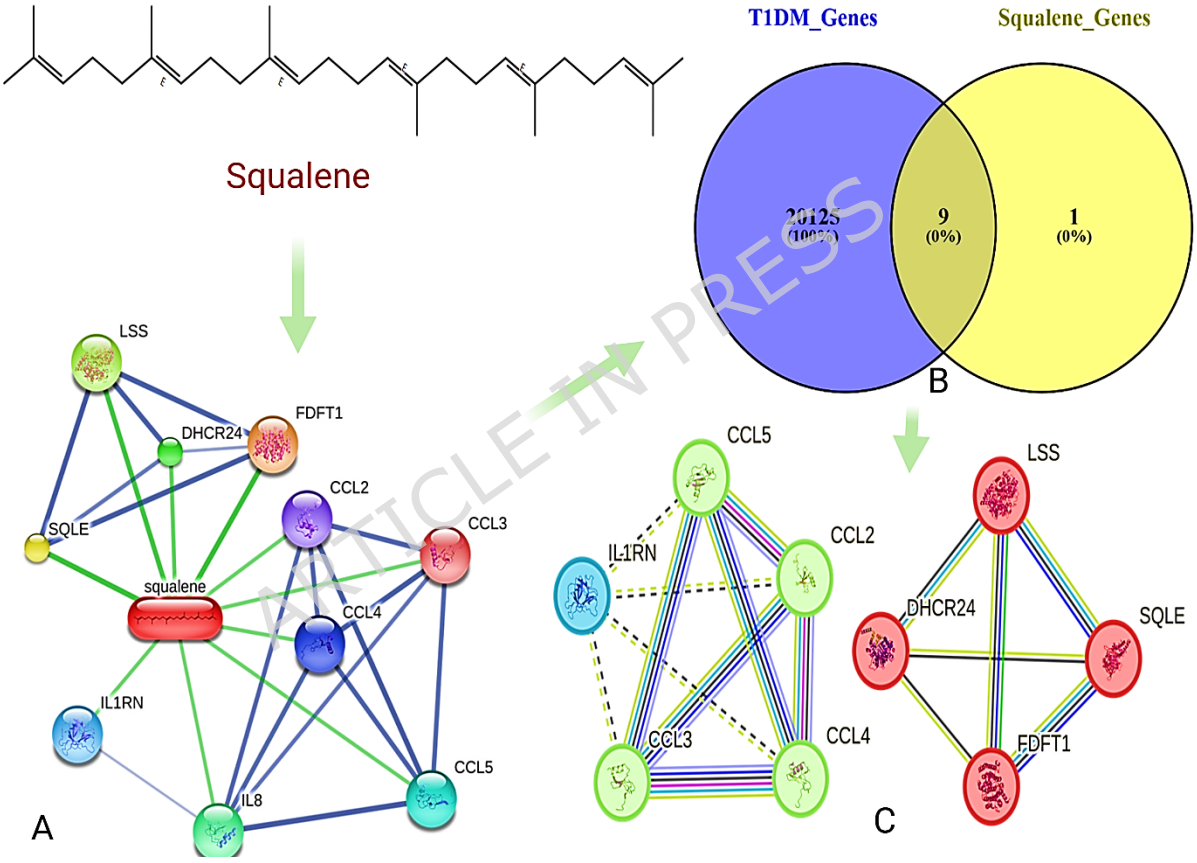

Figure 9: Gene association and clustering analysis. (A) Identified genes associated with squalene. (B) Venn diagram showing common genes between squalene-associated and Type 1 diabetes mellitus-related genes. (C) Clustering analysis of the common genes, grouped into three distinct clusters represented by red, blue, and green colors, each associated with specific gene sets.

3.10. Molecular Docking

Squalene was docked into the active site of the squalene epoxidase protein (SQLE; PDB ID: 6C6N, chain A) using AutoDock, yielding a binding affinity of –10.34 kcal/mol. This value was comparable to that of the co-crystallized ligand NB-598, which showed a score of –11.14 kcal/mol, suggesting that squalene may engage the protein with similar binding strength. The docking results revealed polar interactions with Thr417, Gln168, and His522, as well as negatively charged contacts with Glu165 and Glu323. Hydrophobic residues such as Val163, Phe166, Tyr195, Ile197, Met421, Pro415, Leu416, Leu324, Ala322, Leu345, Phe306, Tyr210, Ile208, Val506, Pro505, Val526, Cys491, Tyr494, Phe495, Phe523, Leu469, Leu509, and Leu518 also contributed to the binding **(Figure 10)**. Flexible residues Gly418 and Gly420 were positioned near the ligand, potentially aiding in pocket adaptability. Several of these residues including Glu165, His522, Leu416, Met421, Phe495, and Phe523 are consistent with those reported in crystallographic studies as important for substrate or inhibitor recognition in SQLE.

The co-crystal ligand NB-598 is known to bind within the hydrophobic substrate pocket of SQLE, forming interactions with residues such as Tyr195, Phe166, Leu324, Leu333, Leu345, Leu416, and Phe477. In the current study, squalene also occupied this same binding pocket, establishing overlapping interactions with Tyr195, Phe166, Phe306, Leu324, Leu333, Leu416, Leu469, and Phe477 (**Figure 10**). Both ligands shared polar contacts with Thr417, Gln168, and His522, while Glu323 was a common stabilizing residue. Glycine residues like Gly418 were also conserved. These observations confirm that squalene binds within the functional cavity defined in the crystal structure[42], supporting the idea that it may modulate SQLE activity by engaging structurally and functionally relevant residues involved in cholesterol biosynthesis and metabolic control.

To further explore the immunomodulatory relevance of squalene, molecular docking was also performed against the IL1R1 receptor (PDB

ID: 1ITB). The docking score was –6.51 kcal/mol, reflecting favorable binding within the known receptor interface. Although 1ITB lacks a co-crystallized ligand, literature-based structural analyses have mapped the interaction region between IL1R1 and its natural ligand IL1β. In this context, squalene formed polar interactions with Asn129 and Ser125, and engaged negatively charged residues Glu128 and Glh129. It also formed electrostatic interactions with Lys63 and Arg25. Hydrophobic contacts included residues such as Phe133, Val132, Pro131, Met130, Ala127, and Tyr127, as well as Pro26, Pro28, and Leu29, which create a stable hydrophobic environment around the ligand (**Figure 10**). These residues, particularly Tyr127, Glu128, Asn129, Ser125, Phe133, and Met130, are reported in previous structural studies as part of the canonical binding region for IL1β[41]. The overlap between reported and observed residues supports that squalene binds within the functional domain of IL1R1. This suggests that it may directly influence IL1R1 signaling by targeting key residues essential for receptor-ligand recognition.

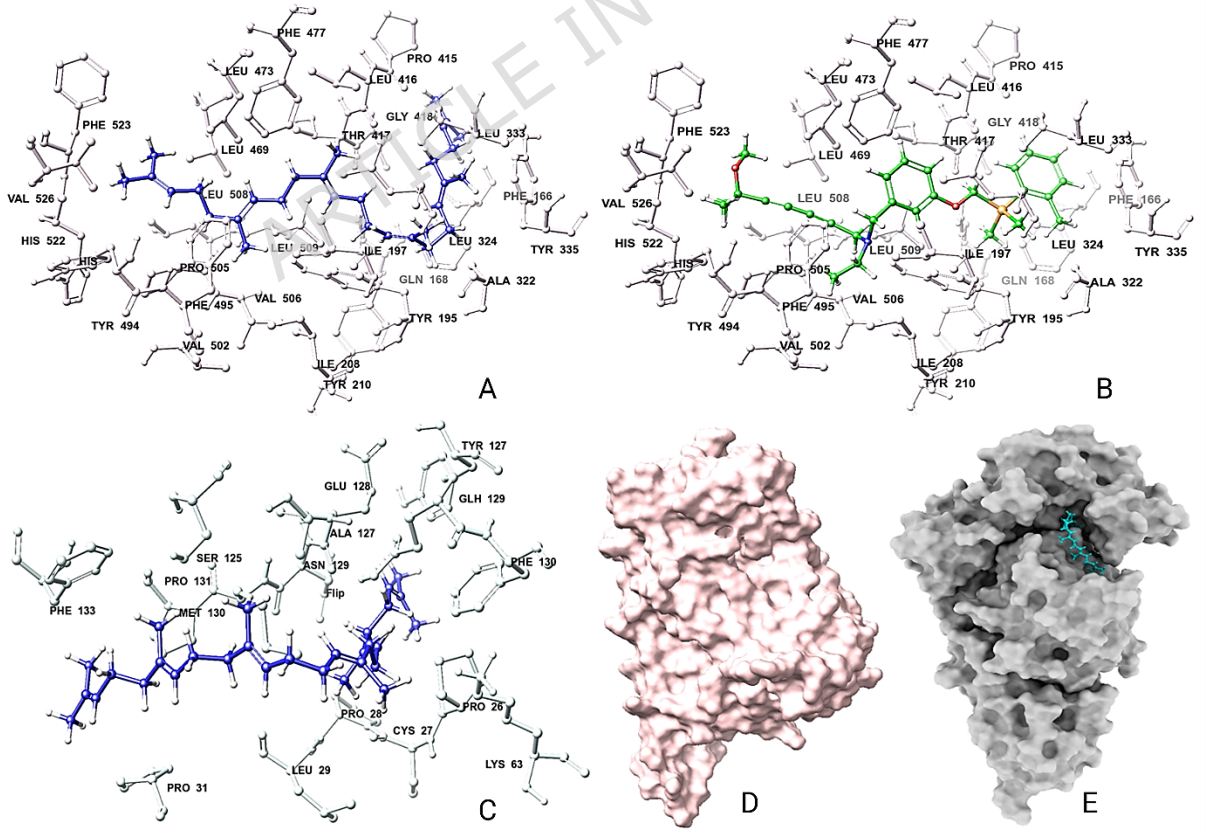

Figure 10: 3D interaction diagrams of protein–ligand complexes. (A) Squalene bound to SQLE protein; (B) co-crystal ligand bound to SQLE; (C) squalene interaction with IL1R1; (D) surface representation of SQLE with bound ligand; (E) surface representation of IL1R1 with bound ligand.

4. Discussion

This study investigated the antidiabetic effects of squalene in an alloxan-induced model of Type 1 Diabetes Mellitus (T1DM). Alloxan selectively damages pancreatic β-cells and impairs insulin secretion, producing a diabetic phenotype that mirrors autoimmune-mediated hyperglycemia in humans[46]. The findings showed that squalene treatment improved multiple diabetic parameters, including glucose regulation, insulin secretion, lipid metabolism, glycogen storage, renal and hepatic biomarkers, oxidative stress markers, and proinflammatory cytokine levels. These outcomes were further contextualized using systems-level network pharmacology analysis, which provided insight into the molecular targets and pathways potentially modulated by squalene. The improvements observed *in vivo* strongly align with the *in-silico* predictions. The high binding affinity of squalene toward SQLE corresponds with the observed normalization of cholesterol and triglyceride levels. Likewise, the interaction of squalene with IL1R1 is supported by the marked reduction in IL-1β, IL-6, and TNF-α levels. Enrichment of chemokine-related pathways (CCL2, CCL3, CCL4, CCL5) corresponds with suppressed inflammation in vivo. This integrated interpretation strengthens the mechanistic relevance of the biochemical outcomes.

The significant weight loss observed in alloxan-induced diabetic rats likely resulted from catabolic stress, dehydration, and impaired glucose utilization due to β-cell dysfunction[47]. Squalene treatment preserved body weight, suggesting a protective effect against metabolic wasting. This aligns with restored hepatic glycogen levels, indicating improved glucose storage capacity.

Hyperglycemia-induced glycation of hemoglobin leads to elevated HbA1c levels, a reliable marker of chronic blood glucose elevation. Squalene

significantly reduced HbA1c levels, especially at higher doses, indicating long-term glycemic control. Restoration of insulin levels and reduction in serum amylase further supported the preservation of β-cell function[18]. These effects are consistent with previous studies in streptozotocin-induced diabetic models, where squalene lowered blood glucose and preserved pancreatic tissue.[20] The lipid profile of diabetic rats showed increased total cholesterol and triglycerides, and reduced HDL characteristics of diabetic dyslipidemia that contribute to cardiovascular complications. Treatment with squalene normalized lipid levels, suggesting beneficial effects on lipid metabolism. Supporting this, computational analysis identified key squalene targets (SQLE, DHCR24, FDFT1, LSS) involved in cholesterol biosynthesis[48–50]. These enzymes are regulated by the SREBP transcriptional system, which is essential for maintaining lipid homeostasis. Enrichment of SREBP signaling and cholesterol biosynthesis pathways in Reactome and KEGG further supports this mechanism.

To provide structural evidence for this mechanism, molecular docking was performed with the human squalene epoxidase enzyme (SQLE; PDB ID: 6C6N). Squalene exhibited a strong binding affinity (–10.34 kcal/mol), closely comparable to the co-crystal ligand NB-598 (–11.14 kcal/mol). It formed interactions with key residues including Thr417, Gln168, His522, Glu165, Glu323, and numerous hydrophobic residues such as Phe166, Tyr195, Leu324, Leu416, and Phe477. These residues are consistent with those reported in crystallographic studies to be essential for inhibitor binding[42]. The shared binding cavity and residue overlap strongly support squalene's ability to engage SQLE directly and modulate cholesterol biosynthesis. Renal dysfunction, as indicated by elevated serum creatinine levels in diabetic rats, was alleviated by squalene, suggesting renal protection. Oxidative stress, a common feature in diabetes, was evident from increased malondialdehyde and reduced levels of glutathione, superoxide dismutase, and catalase. Squalene treatment restored antioxidant defenses, consistent with previous reports of its antioxidative effects in diabetic and cardiovascular contexts[18,19]. Hyperglycemia-

induced oxidative stress can cause pancreatic acinar cell injury, resulting in leakage of amylase into circulation. The significant reduction in amylase levels following squalene administration suggests that its antioxidant action may protect acinar cell integrity and mitigate pancreatic injury.

Squalene also demonstrated anti-inflammatory activity by reducing proinflammatory cytokines such as IL-1β, IL-6, and TNF-α. Network pharmacology findings complemented these results by identifying immune-related targets such as IL1RN and CCL chemokines (CCL2, CCL3, CCL4, CCL5) enriched in pathways linked to immune cell chemotaxis and cytokine production. Gene Ontology enrichment highlighted strong associations with monocyte, neutrophil, and macrophage chemotaxis, key processes involved in the recruitment of immune cells during autoimmune β-cell destruction. To further explore this anti-inflammatory mechanism, molecular docking analysis was conducted against the interleukin-1 receptor type 1 (IL1R1; PDB ID: 1ITB). Squalene exhibited a binding score of –6.51 kcal/mol and interacted with key residues including Asn129, Ser125, Glu128, Lys63, Arg25, Phe133, and Met130. Many of these residues are located within the canonical ligand-binding interface identified in structural studies of IL1R1. The overlap suggests that squalene may modulate IL1β signaling by binding to the receptor's functional site, providing a structural rationale for the observed reduction in inflammatory cytokines[41].

The involvement of CCR2 and CCR5 receptor binding further suggests that squalene may influence immune signaling checkpoints relevant to islet inflammation. STRING-based clustering revealed two distinct modules. One included chemokine mediators involved in immune cell trafficking, and the other contained cholesterol biosynthesis enzymes. K-means decomposition identified three functionally distinct clusters: (1) CCL chemokines mediating immune cell recruitment, (2) cholesterol biosynthetic enzymes suggesting metabolic regulation, and (3) IL1RN, which clustered independently, indicating a separate anti-inflammatory role. IL1RN is a natural inhibitor of IL-1 signaling and has been studied in

autoimmune diabetes for its ability to suppress islet inflammation. Pathway enrichment from Reactome and WikiPathways further identified IL-10 signaling, Toll-like receptor signaling, and IL-18 signaling as potential immunoregulatory routes influenced by squalene. The independent clustering of IL1RN suggests that squalene may also exert immunomodulatory effects beyond chemokine regulation. The predicted involvement of IL-10 signaling, known for promoting immune tolerance and reducing Th1/Th17-driven inflammation, offers additional support for squalene's potential to modulate inflammatory responses in T1DM. Thus, the in vivo results provide evidence that squalene improves multiple diabetic outcomes. Computational analysis supports these findings by identifying relevant molecular targets and pathways. The combined immunological and metabolic effects observed in this study indicate that squalene may be a promising candidate for modulating both β-cell inflammation and systemic metabolic imbalance in autoimmune diabetes. Further preclinical and clinical investigations will be necessary to evaluate its therapeutic potential.

Limitations and Future Perspectives

While this study provides comprehensive evidence for the therapeutic potential of squalene in managing hyperglycemia, dyslipidemia, inflammation, and oxidative stress in a rodent model of type 1 diabetes, several limitations should be noted. The use of alloxan-induced diabetes primarily reflects β-cell destruction and may not capture the full spectrum of autoimmune responses involved in human type 1 diabetes. Additionally, the mechanistic insights derived from network pharmacology are predictive and require further validation through molecular and cellular assays. Molecular dynamics (MD) simulations were not performed to assess the stability and time-dependent behavior of squalene–target interactions, which represents a limitation of the *in-silico* analysis. Although squalene showed multi-target efficacy, its pharmacokinetic profile, tissue distribution, and long-term safety were not evaluated in this study. The study did not assess enzymes involved in cholesterol

metabolism (e.g., HMG-CoA reductase), which may provide additional mechanistic clarity. Additionally, the present study did not include gene- or protein-expression assays, nor were histopathological examinations of pancreatic or hepatic tissues performed.

Although the biochemical findings strongly indicate antioxidant, anti-inflammatory, and metabolic regulatory effects of squalene, future studies should incorporate molecular and histological analyses to validate the mechanistic pathways proposed using gene expression and protein-level studies in pancreatic, hepatic, and immune tissues. Investigating squalene's effects in autoimmune diabetes models, such as NOD mice, may provide more clinically relevant insights. Furthermore, evaluating its potential in combination with standard antidiabetic therapies could help determine additive or synergistic effects. Future studies should integrate molecular dynamics simulations to complement docking analyses and provide insights into the stability and conformational dynamics of squalene-protein complexes. Clinical studies assessing efficacy, safety, and dosing strategies will be critical for translating these findings into therapeutic applications.

Conclusion

This study demonstrates that squalene improved glycemic control, restored serum insulin levels, normalized the lipid profile, enhanced liver glycogen content, and ameliorated renal dysfunction in alloxan-induced diabetic rats. Squalene also lowers proinflammatory cytokine levels, indicating an overall improvement in inflammatory status. The integration of experimental data with network pharmacology analysis reveals that squalene targets key regulators of cholesterol metabolism and inflammatory pathways, including SREBP-mediated lipid signaling and IL1RN-linked cytokine modulation. Molecular docking further supports these findings by confirming that squalene directly binds to the catalytic pocket of SQLE with a high binding affinity and engages functionally important residues associated with cholesterol biosynthesis. Similarly, docking against IL1R1 identified key interface residues involved in ligand

recognition, suggesting squalene may also modulate IL1β-mediated inflammatory signaling. These findings establish the therapeutic relevance of squalene in managing diabetes and complications through combined metabolic and immune pathway modulation.

Funding:

Not Applicable

Data availability

All data generated or analysed during this study are included in this published article and its supplementary information files. Protein structures used for molecular docking were obtained from the Protein Data Bank (PDB), and target information was retrieved from publicly available databases such as UniProt. No new protein sequences, gene expression datasets, or macromolecular structures were generated during this study.

References

1. Antar, S. A. *et al.* Diabetes mellitus: Classification, mediators, and complications; A gate to identify potential targets for the development of new effective treatments. *Biomed. Pharmacother.* **168**, 115734 (2023).
2. Yang, T. *et al.* An update on chronic complications of diabetes mellitus: from molecular mechanisms to therapeutic strategies with a focus on metabolic memory. *Mol. Med.* **30**, 1–19 (2024).
3. Usman, M. S., Khan, M. S. & Butler, J. The Interplay Between Diabetes, Cardiovascular Disease, and Kidney Disease. *Compendia* **2021**, 13-18 (2021).
4. Rao, G. H. R. Cardiometabolic diseases: Risk factors and novel approaches for the management of risks. *Cardiometabolic Dis.* 3-26 (2025) doi:10.1016/B978-0-323-95469-3.00022-X.

5. Caturano, A. *et al.* Oxidative Stress and Cardiovascular Complications in Type 2 Diabetes: From Pathophysiology to Lifestyle Modifications. *Antioxidants* **14**, (2025).
6. Islam, K. *et al.* Diabetes Mellitus and Associated Vascular Disease: Pathogenesis, Complications, and Evolving Treatments. *Adv. Ther.* **42**, 2659–2678 (2025).
7. Guo, H., Wu, H. & Li, Z. The Pathogenesis of Diabetes. *Int. J. Mol. Sci.* **24**, 6978 (2023).
8. Iheagwam, F. N. & Iheagwam, O. T. Diabetes mellitus: The pathophysiology as a canvas for management elucidation and strategies. *Med. Nov. Technol. Devices* **25**, 100351 (2025).
9. Lima, J. E. B. F., Moreira, N. C. S. & Sakamoto-Hojo, E. T. Mechanisms underlying the pathophysiology of type 2 diabetes: From risk factors to oxidative stress, metabolic dysfunction, and hyperglycemia. *Mutat. Res. Toxicol. Environ. Mutagen.* **874–875**, 503437 (2022).
10. Association, A. D. 2. Classification and Diagnosis of Diabetes: Standards of Medical Care in Diabetes-2021. *Diabetes Care* **44**, S15–S33 (2021).
11. Sami, A. *et al.* Genetics of diabetes and its complications: a comprehensive review. *Diabetol. Metab. Syndr.* **17**, 1–21 (2025).
12. Westman, E. C. Type 2 Diabetes Mellitus: A Pathophysiologic Perspective. *Front. Nutr.* **8**, 707371 (2021).
13. Redondo, M. J. & Morgan, N. G. Heterogeneity and endotypes in type 1 diabetes mellitus. *Nat. Rev. Endocrinol.* **19**, 542–554 (2023).
14. Tan, S. Y. *et al.* Type 1 and 2 diabetes mellitus: A review on current treatment approach and gene therapy as potential intervention. *Diabetes Metab. Syndr. Clin. Res. Rev.* **13**, 364–372 (2019).
15. Shahzad, A. *et al.* Integrated in vitro, in silico, and in vivo approaches to elucidate the antidiabetic mechanisms of Cicer arietinum and Hordeum vulgare extract and secondary metabolites. *Sci. Reports* **15**, 1–26 (2025).
16. Saini, T. *et al.* Role of bioactive phytochemicals in plant seeds and

leaves for diabetes control and prevention: a comprehensive review. *Phytochem. Rev. 2025* 1–26 (2025) doi:10.1007/S11101-025-10065-1.

17. Lozano-Grande, M. A., Gorinstein, S., Espitia-Rangel, E., Dávila-Ortiz, G. & Martínez-Ayala, A. L. Plant Sources, Extraction Methods, and Uses of Squalene. *Int. J. Agron.* **2018**, 1829160 (2018).
18. Cheng, L., Ji, T., Zhang, M. & Fang, B. Recent advances in squalene: Biological activities, sources, extraction, and delivery systems. *Trends Food Sci. Technol.* **146**, 104392 (2024).
19. Ibrahim, N. I. & Mohamed, I. N. Interdependence of anti-inflammatory and antioxidant properties of squalene–implication for cardiovascular health. *Life* **11**, 1–19 (2021).
20. Widyawati, T., Syahputra, R. A., Syarifah, S. & Sumantri, I. B. Analysis of Antidiabetic Activity of Squalene via In Silico and In Vivo Assay. *Mol.* **28**, 3783 (2023).
21. Marino, F. *et al.* Streptozotocin-Induced Type 1 and 2 Diabetes Mellitus Mouse Models Show Different Functional, Cellular and Molecular Patterns of Diabetic Cardiomyopathy. *Int. J. Mol. Sci.* **24**, (2023).
22. Athmuri, D. N. & Shiekh, P. A. Experimental diabetic animal models to study diabetes and diabetic complications. *MethodsX* **11**, 102474 (2023).
23. Matsuura, Y. *et al.* Altered glucose metabolism and hypoxic response in alloxan-induced diabetic atherosclerosis in rabbits. *PLoS One* **12**, e0175976 (2017).
24. Kottaisamy, C. P. D., Raj, D. S., Prasanth Kumar, V. & Sankaran, U. Experimental animal models for diabetes and its related complications-a review. *Lab. Anim. Res.* **37**, 1–14 (2021).
25. Zou, Y., Zhang, H., Bi, F., Tang, Q. & Xu, H. Targeting the key cholesterol biosynthesis enzyme squalene monooxygenasefor cancer therapy. *Front. Oncol.* **12**, (2022).
26. Zhukova, J. V., Lopatnikova, J. A., Alshevskaya, A. A. & Sennikov, S. V. Molecular mechanisms of regulation of IL-1 and its receptors.

Cytokine Growth Factor Rev. **80**, 59–71 (2024).

27. Yamashita, A. *et al.* Abstract 550: Alteration of Glycolysis Metabolite Levels and Impaired Hypoxic Response in Diabetic Atherosclerosis. *Arterioscler. Thromb. Vasc. Biol.* **37**, (2017).
28. Matsuda, M., Komiyama, Y., Suzuki, T. & Moriyama, M. Effect of Rapid Centrifugation Using High Centrifugal Force on Procoagulant Activity in Plasma Samples. *Clin. Lab.* **68**, 2422–2427 (2022).
29. Soni, L. K. *et al.* In vitro and in vivo antidiabetic activity of isolated fraction of Prosopis cineraria against streptozotocin-induced experimental diabetes: A mechanistic study. *Biomed. Pharmacother.* **108**, 1015–1021 (2018).
30. Senthilkumar, M., Amaresan, N. & Sankaranarayanan, A. Estimation of Superoxide Dismutase (SOD). 117–118 (2021) doi:10.1007/978-1-0716-1080-0_29.
31. Yuan, L. *et al.* A rapid colorimetric method for determining glutathione based on the reaction between cobalt oxyhydroxide nanosheets and 3,3′,5,5′-Tetramethylbenzidine. *Microchem. J.* **160**, 105639 (2021).
32. Akbari, B., Najafi, F., Bahmaei, M., Mahmoodi, N. M. & Sherman, J. H. Modeling and optimization of malondialdehyde (MDA) absorbance behavior through response surface methodology (RSM) and artificial intelligence network (AIN): An endeavor to estimate lipid peroxidation by determination of MDA. *J. Chemom.* **37**, e3468 (2023).
33. Madiraju, C. *et al.* A Unique Multiplex ELISA to Profile Growth Factors and Cytokines in Cerebrospinal Fluid. *Methods Mol. Biol.* **2612**, 157–168 (2023).
34. Szklarczyk, D. *et al.* STITCH 5: Augmenting protein-chemical interaction networks with tissue and affinity data. *Nucleic Acids Res.* **44**, D380–D384 (2016).
35. Amberger, J. S., Bocchini, C. A., Scott, A. F. & Hamosh, A. OMIM.org: leveraging knowledge across phenotype–gene relationships. *Nucleic Acids Res.* **47**, D1038 (2018).
36. Stelzer, G. *et al.* The GeneCards suite: From gene data mining to

disease genome sequence analyses. *Curr. Protoc. Bioinforma.* **2016**, 1.30.1-1.30.33 (2016).

37. Szklarczyk, D. *et al.* The STRING database in 2021: Customizable protein-protein networks, and functional characterization of user-uploaded gene/measurement sets. *Nucleic Acids Res.* **49**, D605–D612 (2021).
38. Zhou, Y. *et al.* Metascape provides a biologist-oriented resource for the analysis of systems-level datasets. *Nat. Commun.* **10**, 1–10 (2019).
39. Kanehisa, M., Sato, Y., Kawashima, M., Furumichi, M. & Tanabe, M. KEGG as a reference resource for gene and protein annotation. *Nucleic Acids Res.* **44**, D457–D462 (2016).
40. Kanehisa, M., Furumichi, M., Sato, Y., Matsuura, Y. & Ishiguro-Watanabe, M. KEGG: biological systems database as a model of the real world. *Nucleic Acids Res.* **53**, D672–D677 (2025).
41. Vigers, G. P. A., Anderson, L. J., Caffes, P. & Brandhuber, B. J. Crystal structure of the type-I interleukin-1 receptor complexed with interleukin-1β. *Nature* **386**, 190–194 (1997).
42. Padyana, A. K. *et al.* Structure and inhibition mechanism of the catalytic domain of human squalene epoxidase. *Nat. Commun.* **10**, 1–10 (2019).
43. Eberhardt, J., Santos-Martins, D., Tillack, A. F. & Forli, S. AutoDock Vina 1.2.0: New Docking Methods, Expanded Force Field, and Python Bindings. *J. Chem. Inf. Model.* **61**, 3891–3898 (2021).
44. Kohli, K., Pillarisetty, V. G. & Kim, T. S. Key chemokines direct migration of immune cells in solid tumors. *Cancer Gene Ther.* **29**, 10–21 (2021).
45. Picón, D. F. & Skouta, R. Unveiling the Therapeutic Potential of Squalene Synthase: Deciphering Its Biochemical Mechanism, Disease Implications, and Intriguing Ties to Ferroptosis. *Cancers (Basel).* **15**, 3731 (2023).
46. Bansode, T., Salalkar, B., Dighe, P., Nirmal, S. & Dighe, S. Comparative evaluation of antidiabetic potential of partially purified

bioactive fractions from four medicinal plants in alloxan-induced diabetic rats. *Ayu* **38**, 165 (2017).

47. Belhadj, S. *et al.* Metabolic impairments and tissue disorders in alloxan-induced diabetic rats are alleviated by Salvia officinalis L. essential oil. *Biomed. Pharmacother.* **108**, 985–995 (2018).
48. Gu, Y. *et al.* Combinatorial metabolic engineering of Saccharomyces cerevisiae for improved production of 7-dehydrocholesterol. *Eng. Microbiol.* **3**, 100100 (2023).
49. Besnard, T. *et al.* Biallelic pathogenic variants in the lanosterol synthase gene LSS involved in the cholesterol biosynthesis cause alopecia with intellectual disability, a rare recessive neuroectodermal syndrome. *Genet. Med.* **21**, 2025–2035 (2019).
50. Zhou, Y. *et al.* Post-translational switch of DHCR24 acetylation sustains sterol synthesis and promotes HCC via the 7-ketocholesterol/p62 axis. *Cell Rep.* **44**, 116640 (2025).